ACS APPLIED MATERIALS & INTERFACES

Research Article

www.acsami.org

Control of the Metal–Insulator Transition in VO_2 Epitaxial Film by Modifying Carrier Density

F.H. Chen,[†] L. L. Fan,[†] S. Chen,[†] G. M. Liao,[†] Y. L. Chen,[†] P. Wu,[†] Li Song,[†] C. W. Zou,*[,†,§] and Z. Y. Wu*[,†,‡]

[†]National Synchrotron Radiation Laboratory, University of Science and Technology of China, Hefei 230029, P.R. China

[‡]Institute of High Energy Physics, Chinese Academy of Science, Beijing 100049, P.R. China

S *Supporting Information*

ABSTRACT: External controlling the phase transition behavior of vanadium dioxide is important to realize its practical applications as energy-efficient electronic devices. Because of its relatively high phase transition temperature of 68 °C, the central challenge for VO_2-based electronics, lies in finding an energy efficient way, to modulate the phase transition in a reversible and reproducible manner. In this work, we report an experimental realization of p−n heterojunctions by growing VO_2 film on p-type GaN substrate. By adding the bias voltage on the p−n junction, the metal−insulator transition behavior of VO_2 film can be changed continuously. It is demonstrated that the phase transition of VO_2 film is closely associated with the carrier distribution within the space charge region, which can be directly controlled by the bias voltage. Our findings offer novel opportunities for modulating the phase transition of VO_2 film in a reversible way as well as extending the concept of electric-field modulation on other phase transition materials.

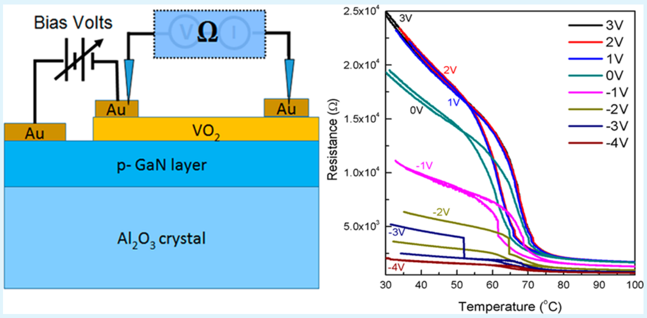

KEYWORDS: *vanadium dioxide, p-GaN, phase transition modulation, carrier concentration*

1. INTRODUCTION

Strongly correlated materials have attracted widespread attention because of the significant changes in physical properties caused by phase transition, which makes these materials of particular interest for their potential device applications such as electrical switches and sensors. As a typical transition metal oxide, VO_2 material shows a first-order reversible metal-to-insulator transition (MIT) with the critical temperature (T_c) of 68 °C. Across the phase transition, the resistance of VO_2 undergoes a large change (up to 5 orders of magnitude) from monoclinic insulating state to a high-temperature metal phase with rutile structure.[1] In addition, the optical transmission also exhibit distinct changes, especially in the infrared region. These excellent characteristics of VO_2 material make it suitable for many promising applications in various fields such as smart windows,[2] optical switching devices,[3] memory materials,[4] photoconductive infrared detectors,[5] and thermal/chemical sensors.[6,7]

However, the critical MIT temperature of 68 °C is still too high to satisfy those practical applications based on VO_2 material. Thus, much effort has been devoted to modulation the phase transition behavior of VO_2 and attempt to tune the T_c close to room temperature. Though the microscopic origin of the MIT is still an open problem, the most recognized models of the transition are based on the strong electron correlation (Mott−Hubbard transition) and electron−lattice coupling (Peierls transition). Accordingly, the possible ways to control the phase transition behavior of VO_2 are mainly focusing on modulating the crystal lattice and the charge/electronic density. In fact, many experiments have been demonstrated that the T_c of VO_2 can be effectively reduced by higher valence metal ions doping,[8−11] by adding internal/external stress,[12−16] or by adding the external electric-field.[17−19]

Adding the bias voltage on VO_2 through an ionic liquid gate is an easy way to examine the effects of electric field on the phase transition behavior. Recently, M. Nakano's group[18] fabricated an electric double-layer transistor (EDLT) based on VO_2 and investigated the electrical switching behavior between the metallic tetragonal phase and the insulating monoclinic phase. They suggested that the electrostatic charging at a surface triggered the motion of localized charge carriers in the bulk material, finally leading to the metallic ground state. Based on similar experiment with ion-liquid, S.S. Parkin group[19] proposed that the electrolyte gating of VO_2 created an electric field−induced oxygen vacancies, decreasing the phase transition temperature. Although there was distinct disagreement between them, two different experiments both pointed out the important role of the electric field on the phase transition

Received: January 18, 2015
Accepted: March 9, 2015
Published: March 9, 2015

DOI: 10.1021/acsami.5b00540
ACS Appl. Mater. Interfaces 2015, 7, 6875–6881

and demonstrated the possibility of a reversible control of the phase transition by an external bias voltage.

It is well-known that within a normal semiconductor p−n junction an internal electric field region occurs due to the diffusion of electron and hole carriers at the interface. The addition of an external bias voltage on the p−n junction may tune the barrier width/depletion layer, a possible way to achieve an efficient control of the carrier/charge density at the interfacial layer. Actually, it has been investigated to form the junction between n-type VO_2 and a p-type conventional semiconductor in previous study, but there still exist some obstacles to fabricate p−n junction with rectifying transport properties owing to crystal symmetry, high work function[20−24] and high carrier densty[25,26] of VO_2. Zhou. et al.[27,28] prepared the VO_2/GaN p−n junction and systematically investigated the interfacial growth behavior, the band offset and minority carrier dynamics, whereas the MIT characteristics and transition mechanism of VO_2 under different bias were not discussed in their experiment.

In the current study, we have prepared high-quality epitaxial VO_2 films on p-GaN layers on sapphire substrates and studied the MIT characteristics under different external bias voltage. Our results indicated that the phase transition of VO_2 thin film can be modulated by the external bias voltage, resulting in the controllable metallic phase at room temperature. This bias-driven phase transition is suggested to be closely associated with the depletion layer at the interface and the carrier density in VO_2 epitaxial film. Our experiment results show that integrating the VO_2 layer onto hetero p−n junction is an ideal model system to better understand the phase transition in VO_2 and explore the feasibility to design electronic/optical devices with new functionalities.

2. EXPERIMENTAL METHODS

The commercially p-type GaN on c-plane sapphire grown by MOCVD was used in this study (Mg-doped, hole concentration $\sim 1.37 \times 10^{17}\,\mathrm{cm}^{-3}$). Prior to the VO_2 deposition, the GaN substrates were ultrasonically cleaned consequently in acetone and isopropanol for 10 min and followed by deionized water rinse. The VO_2 films were grown on this p-GaN (0001) layer by an rf-plasma assisted oxide-MBE instrument working with a base pressure better than 3×10^{-9} Torr. During the deposition, the substrate temperature T_s was maintained at 530 °C and the growth pressure was maintained at 3.2×10^{-5} Torr. The Reflection High Energy Electron Diffraction (RHEED) was used to monitor the whole growth process. The film thickness is controlled by adjusting the deposition time and two samples are prepared with the final thickness of about 25 and 90 nm, respectively. The details of the epitaxial film preparation are reported elsewhere.[29]

The prepared epitaxial thin films were characterized by Raman spectroscopy with a 532 nm excitation laser source. The crystal structure and the growth orientation were characterized by X-ray diffraction (XRD) at the diffraction station at the Shanghai Synchrotron Radiation Facility (SSRF BL14B1 station). The φ-scan XRD were also performed in order to examine the epitaxial growth behavior at the interface. The I−V curve measurements were conducted by Keithley 2410 sourcemeter on a sample stage with variable temperature. The measurements of the electrical resistance vs temperature for all samples were made with a customized four-probe system installed on a variable-temperature sample stage. The external bias voltage was applied to two poles which were contacted with the surface of p-GaN and VO_2, respectively.

3. RESULTS AND DISCUSSION

Figure 1a shows the XRD diffraction in regular θ-2θ scanning mode for the VO_2/p-GaN/Al_2O_3 sample. The peak located at $2\theta = 34.72°$ corresponds to the GaN layer (002) plane, which has been confirmed in previous reports.[28,30] The 2θ peak at 41.68° is attributed to Al_2O_3 (006) diffractions, while the 2θ peak at 39.7° is from the VO_2 (020) or (002) diffraction. There are no other diffraction peaks existed in the XRD curves, indicating the highly oriented growth of the VO_2 epitaxial film. Figure 1b showed the room-temperature Raman scattering curves for the VO_2/p-GaN/Al_2O_3 structure and VO_2/Al_2O_3 structure, respectively. These two spectra coincide with eath other, except for the main peak at 569 and 733 cm^{-1} from the E2 (high) mode and A1 (LO) mode of GaN layer. The peaks at at 194, 223, 264, 307, 338, 387, 440, 498, and 617 cm^{-1} were all from the monoclinc VO_2, indicating the pure M1 phase of the deposited VO_2 film on p-GaN/Al_2O_3 substrate.

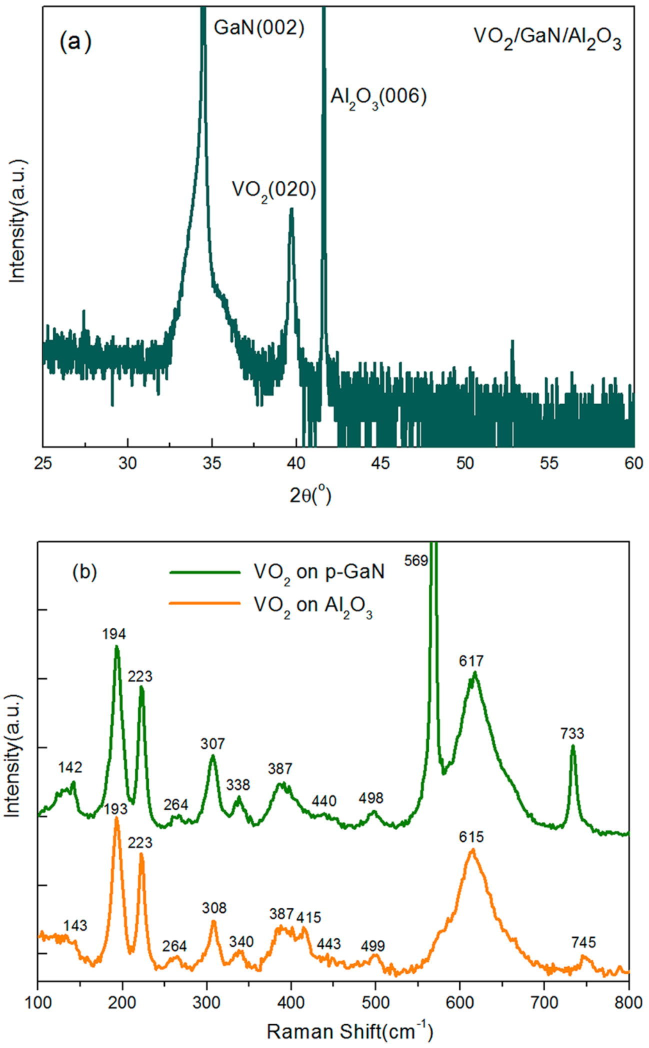

Figure 1. (a) θ−2θ XRD patterns for the VO_2/p-GaN/Al_2O_3 structure; (b) Raman spectra for the VO_2 films on sapphire substrate and GaN/sapphire substrate.

To further examine the epitaxial growth behavire of VO_2 layer onGaN/Al_2O_3 surface, we conducted the φ-scan XRD study. Figure 2a shows the φ-scan patterns of VO_2 (011) GaN (102) and Al_2O_3 (102) plane. In the VO_2 (011) φ-scan spectrum, we clearly detected six peaks due to the 2-fold symmetry along the [020] orientation and the presence of three VO_2 planes: (011), (−111), and (110), rotated by 120° each other. As a consequence, the (−111) and (110) appear in VO_2 (011) φ-scan process due to the approximate Bragg angles and

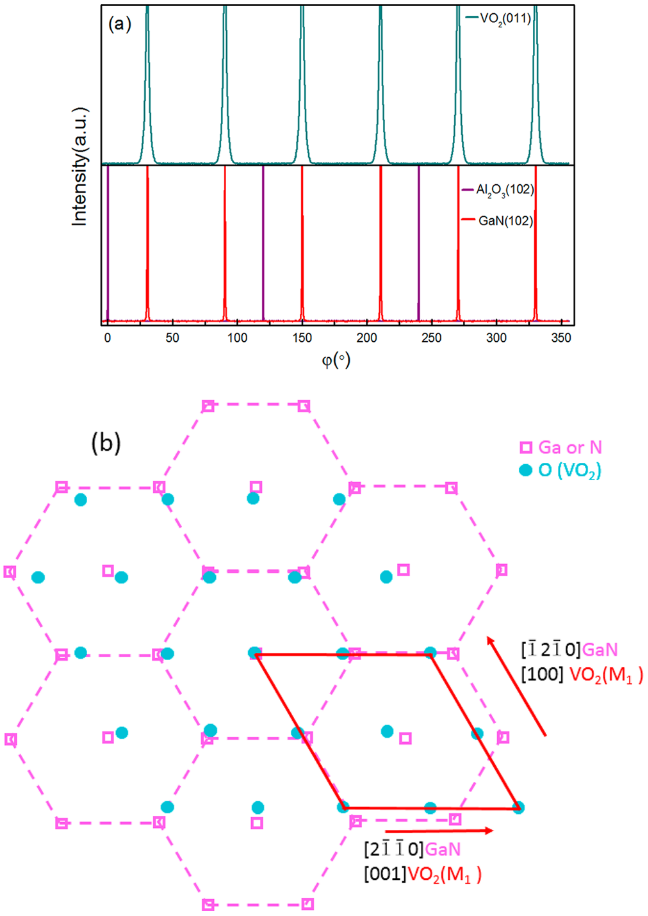

Figure 2. (a) φ-scan XRD from VO$_2$ (011) plane, GaN (102) plane, and Al$_2$O$_3$ (102) plane; (b) relation for the in-plane lattice matching for VO$_2$ film and GaN layer.

pole angles ($2\theta_{110} = 2\theta_{-111} = 26.87°$, $\psi_{110} = \psi_{-111} = 42.9°$) as that of VO$_2$ (020) plane. Though the (020) plane and (002) plane had the same Bragg angle and pole angles, the (110) and (−111) plane could not appear on the hypothesis of the (002) assignment because of the different pole angles ($\psi_{110} = 68.37°$, $\psi_{-111} = 68.74°$, while $\psi_{011} = 45.1°$).[31,32] Furthermore, the diffraction peak resulted from other planes would not occur because of the different Bragg angles. Thus, the assignment of this peak at $2\theta \sim 39.9°$ to (002) can be ruled out and the VO$_2$ (011) φ-scan experiment unambiguously confirm the [020] growth orientation as shown in Figure 1a.

From Figure 2a, it was observed that Al$_2$O$_3$ had 3-fold symmetry, whereas the p-GaN had 6-fold symmetry, both with [001] direction as rotational axis. Besides, there was 30° deviation between the Al$_2$O$_3$ (102) peaks and the GaN (102) peaks in the φ-scan. Moreover, the VO$_2$ (011) peak positions were accorded with the GaN (102) exactly, which suggests that the *a*-axis of VO$_2$ was aligned with the *b*-axis of GaN lattice. Accordingly, the lattice interface matching relation could be written as Al$_2$O$_3$ [−12−10]//GaN [0−110], Al$_2$O$_3$ [10−10]//GaN [2−1−10] or Al$_2$O$_3$ [11−20]//GaN [0−110], Al$_2$O$_3$ [1−100]//GaN [2−1−10] and VO$_2$ [100]//GaN [-12−10], VO$_2$ [001]//GaN [2−1−10]. The conclusions were consistent with the previous work[28] and did demonstrate the epitaxial growth at the interface for VO$_2$/p-GaN/Al$_2$O$_3$ structure. Furthermore, the X-ray Reflectometry (XRR, see the Supporting Information, Figure 1s) results showed clear oscillation peaks for the VO$_2$/p-GaN/Al$_2$O$_3$ structure, further confirming the high quality of the epitaxial film as well as the p−n jucntion.

The electric properties of the VO$_2$/p-GaN/Al$_2$O$_3$ samples were obtained measuring the temperature dependent *I*−*V* curves of the p−n junctions. The insert in Figure 3a showed the measurement geometric scheme of VO$_2$/p-GaN heterojunction. The gold electrodes were deposited on GaN and VO$_2$ surface and the bias voltage was added for *I*−*V* testing. The *I*−*V* curves plotted in Figure 3a were measured for the n-VO$_2$/p-GaN junction at 30 and 100 °C, corresponding to temperatures before and after the phase transition of the VO$_2$ layer. Other *I*−*V* curves corresponding to different temperatures are showed in Figure 3b and it could be observed that all *I*−*V* curves showed clear rectifying behaviors within the testing temperature region. Furthermore, it was observed that the current increased greatly when the temperature was over the transition temperature (T_c). These phenomena should be related to the semiconductor to metal phase transition of VO$_2$ across the T_c. When the

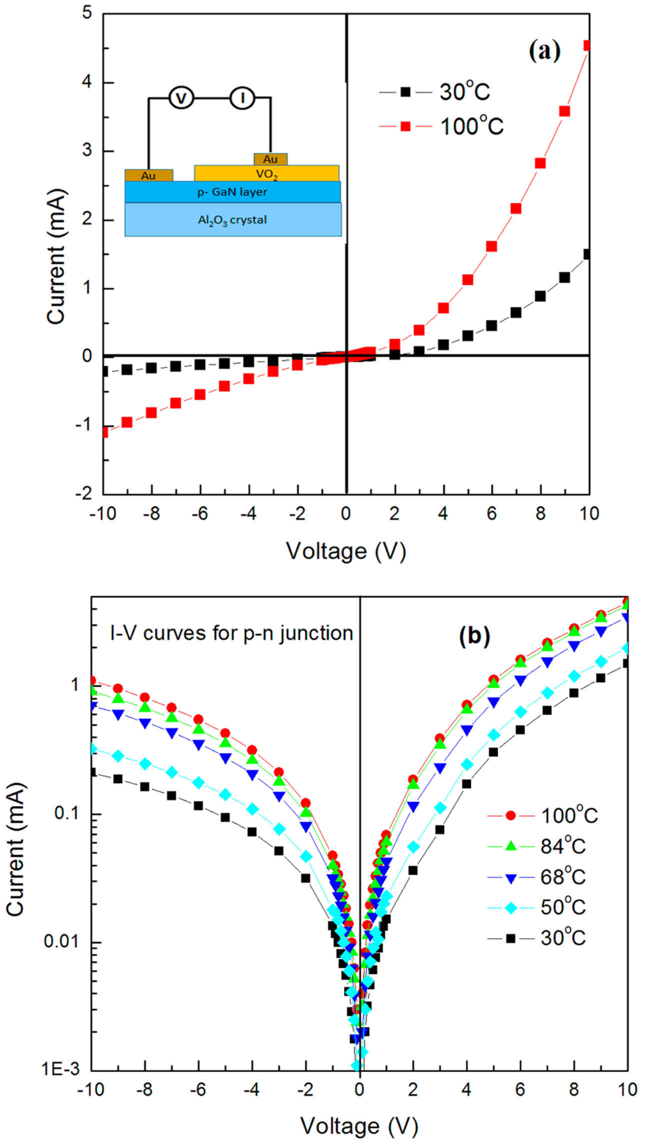

Figure 3. (a) *I*−*V* curves recorded at 30 and 100 °C, the inset shows the configuration of the measurement; (b) *I*−*V* curves recorded across the phase transition of VO$_2$ layer.

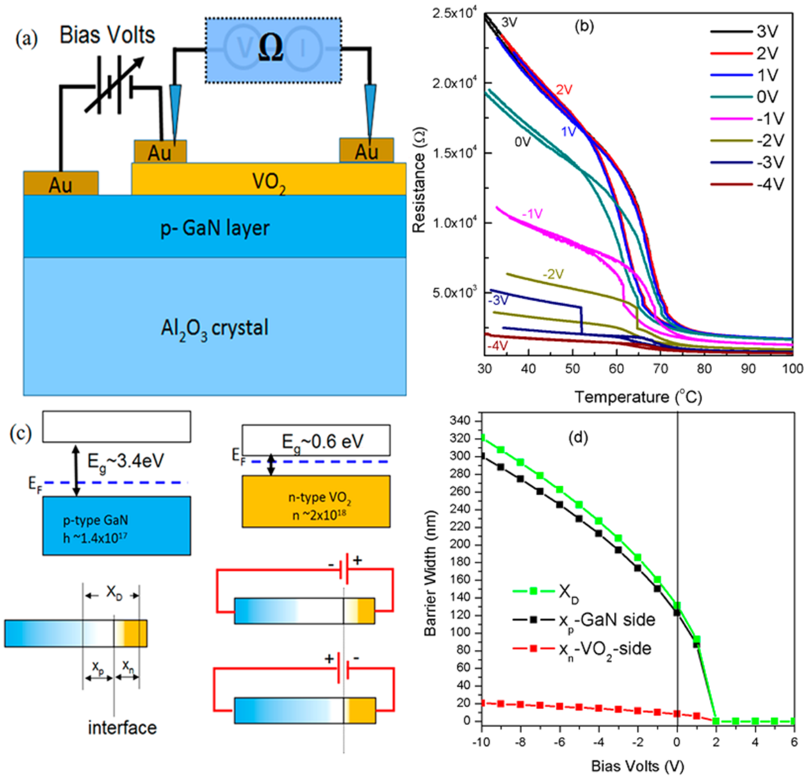

Figure 4. (a) Scheme for the electric measurement; (b) resistance as the function of temperature for 25 nm thick VO_2 layer under different bias voltages; (c) band structure of p-GaN and n-VO_2 as well as the formation of p−n junction; (d) the barrier width/depletion layer as the function of bias volts.

temperature increased over the critical temperature, the p−n junction was almost degenerated to metal/semiconductor junction as a Schottky contact. In addition, we noted that the current−voltage curve were not exponential but nearly linear at large forward bias above T_c, which should be due to the considerable bulk p-GaN resistance dominating the whole p−n junction beyond the critical temperature.

For the VO_2/GaN p−n junction, there existed a barrier layer/depletion layer located at the interface. The barrier width as well as the carrier concentration at the interface could be adjusted by adding the forward or inverse bias voltage. Resultantly, in the n-type VO_2 epitaxial film, the electron carrier density could be changed as the function of the adding voltage, which should play an important role on the phase transition behavior of VO_2 layer. To testing this assumption, we did the VO_2 resistance measurement as the function of temperature under different bias voltages. The testing scheme is shown in Figure 4a. The obtained resistance vs temperature curves were plotted in Figure 4b with the bias voltages from 3.0 V to −4.0 V. It was observed that when the inverse volts were added, the profile of the R−T curves changed greatly. The phase transition behavior was weakened and the total resistance of VO_2 was decreased to close to the metallic phase at room temperature. However, when the forward volts less than 3.0 V were added, the phase transition related R−T curves showed little differences. From these phase transition testing with external bias volts, it was suggested that the phase transition behavior could be easily modulated by the reverse voltages added on the p−n junction.

This phase transition modulation should be directly associated with the internal electric field as well as the carrier density variation located at the depletion layer. Figure 4 (c) shows the band structure of p-GaN, the n-VO_2 and the formation of p−n junction based on them. The X_D is for the total barrier width at the p−n junction interface, whereas the x_p and x_n are for the depletion layer in p-GaN side and VO_2 side, respectively. By Hall measurement at room temperature, the electron concentration for the prepared VO_2 is about $1.2 \times 10^{18}/\text{cm}^3$ to $3.4 \times 10^{18}/\text{cm}^3$, which is quite close to the reported value of $n_i \approx 2 \times 10^{18}/\text{cm}^3$ in VO_2 layer.[27] Considering the hole carrier concentration of $n_p \approx 1.37 \times 10^{17}/\text{cm}^3$ in the commercial GaN substrate, the barrier width/depletion layer can be calculated according to the following three fomula:

$$\text{the total barrier width: } X_D = \left[\frac{2\varepsilon_1\varepsilon_2(n_i + n_p)^2(V_D - V)}{en_in_p(\varepsilon_1 n_p + \varepsilon_2 n_i)}\right]^{1/2} \quad (1)$$

$$\text{the barrier width in VO2: } x_n = \left[\frac{2\varepsilon_1\varepsilon_2 n_p(V_D - V)}{en_i(\varepsilon_1 n_p + \varepsilon_2 n_i)}\right]^{1/2} \quad (2)$$

$$\text{the barrier width in GaN: } x_p = \left[\frac{2\varepsilon_1\varepsilon_2 n_i(V_D - V)}{en_p(\varepsilon_1 n_p + \varepsilon_2 n_i)}\right]^{/2} \quad (3)$$

where the V_D is the contact potential difference, the V is the added bias volts. The n_p and n_i, ε_1 and ε_2 are the carrier concentrations and dielectric constants for GaN and VO_2 layer, respectively. From the work function of 5.2 eV for VO_2 and 7.5 eV for p-GaN, we can estimate the V_D for the p-GaN/VO_2

junction to be 2.3 eV. The dielectric constant is 30−40 for VO_2 and 9.5 for p-GaN according to previous literature.[27] Thus, based on the formula, the carrier width/depletion layer as the function of bias volts are plotted in Figure 4d. From the plot, it can be observed that the barrier width/depletion layer is closely associated with the added bias voltage, especially within the inverse volts range. When the forward bias volts are added, the barrier width/depletion layer will be decreased greatly and disappeared after overcoming the ∼2.0 eV energy-barrier.

Because the VO_2 phase transition process is the main interest, we pay more attention on the VO_2 side of the p-GaN/VO_2 junction. From Figure 4d, it is clear that the depletion layer in VO_2 is up to the maximum depth of 20 nm when adding −10.0 V on the p−n junction. Accordingly, for the epitaxial VO_2 thin film (the thickness ∼ 25 nm), when we add the inverse bias volt up to 10.0 V, the total VO_2 film will be under the control of the internal electric field. As a result, the VO_2 film is completely involved in the depletion layer at the interface due to the carrier diffusion under the unbalance situation. Accordingly, for the first VO_2/GaN sample with the thickness of ∼25 nm, the adding inverse bias voltage has pronounced effect on its phase transition behavior considering the barrier width, just as showing in Figure 4 (b). It can be observed that the resistance is very sensitive to the bias voltage. When −4.0 V inverse bias volt is added, the resistance of VO_2 layer is dropped greatly and almost showing the metallic states at room temperature.

However, for the thicker VO_2 film (the second sample with the thickness of ∼90 nm) on p-GaN, the resistance as the function of temperature is plotted in Figure 5a. It can be observed that the phase transition behavior is still affected by the added bias voltage, although it is not so sensitive. Even under the inverse bias voltage of −15.0 V, the $R-T$ curve still shows the clear hysteretic loop for its phase transition behavior. It is understandable since for the thicker VO_2 layer, the depletion layer at the interface is not dominating the whole VO_2 film when the inverse bias voltage is added according to the curve shown in Figure 4d. Figure 5b shows the resistance jumping behavior of this sample from high resistance to low resistance when −5.0 V inverse voltage is adding. It can be observed that the switching effect is pronounced and reproducible, which should be useful for the practical applications such as logic circuit, sensor or memory.

From the above results, it is suggested that the transition behavior of VO_2 film can be regulated by varying the depletion region controlled by the external inverse voltage added on the p-GaN/VO_2 p−n junction. As it is well-known, VO_2 is a transition metal oxide with a d^1 electron configuration and a band gap of ∼0.6 eV, so the majority carrier of the intrinsic VO_2 layer is electron. When the VO_2 film depositing on p-GaN layer, the p−n junction will be formed (see the Supporting Information, Figure 2s), which will be controlled by the forward bias and the reverse bias voltage. The internal barrier will be produced at the interface since a large number of hole carrier from p-GaN and a lot of electron carrier from VO_2 have diffused each other at the interface of VO_2/p-GaN. Resultantly, the internal electric field is built near the interface of VO_2/p-GaN and hindered the spread of the majority carrier. Finally, the diffusion reaches the equilibrium state because of the balance between the thermal motion and the internal electric field, which means that the depletion layer has been formed. So the width of the depletion layer can be controlled by the extenal field bias.

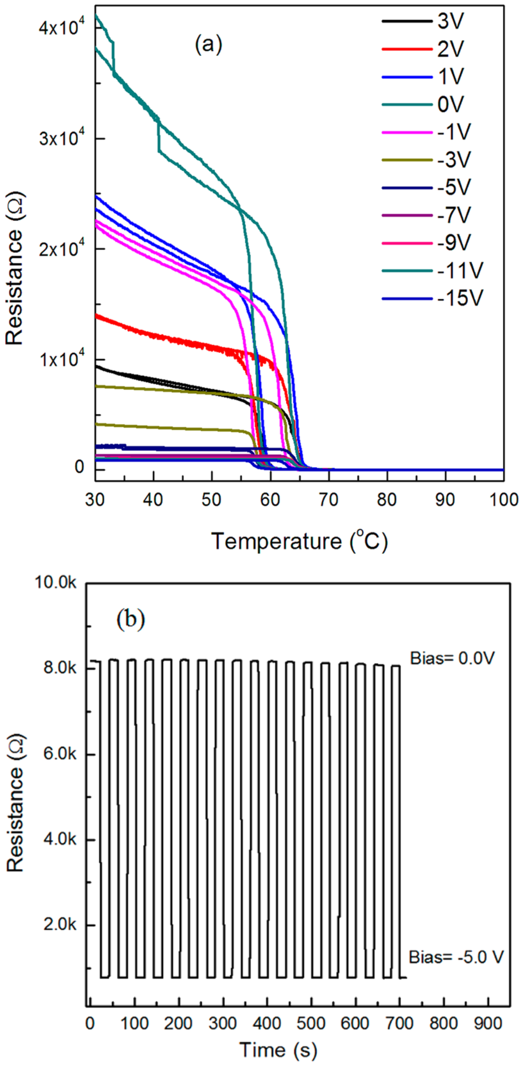

Figure 5. (a) Resistance as the function of temperature for 90 nm thick VO_2 layer under different bias voltages; (b) VO_2 layer shows the switching behavior from high resistance to low resistance when adding the −5.0 V bias voltage.

When focusing on the epitaxial VO_2 thin film on p-GaN layer, its phase transition should be closely associated with the charge/carrier density. In fact, some previous literatures have reported the effects of charge carriers concentration on the phase transition modualtion of VO_2 material,[33] indicating that the carriers intensity does promote the metallic/rutile phase. The ion-liquid assisted VO_2−FET devices also demonstrated that the electrostatic charging at a surface drives all the previously localized charge carriers in the bulk material into motion, leading to the emergence of a three-dimensional metallic ground state.[18] In our current experiment, we achieved the electron density control by the bias voltage adding on p−n junction. When the inverse bias volt is added, the localized electrons in VO_2 thin film will be moved toward GaN side. Consequently, it can be observed that adding the higher inverse bias will induce more pronounced resistance decreasing of the VO_2 film, and finally result into the final metallic-like phase. On the other hand, if the forward bias voltage is added and overcoming the energy-barrier at the interface, the internal electric field at the interface is dissappeared, which has no obvious effect on delocalizing the electrons in VO_2 layer. Thus, the phase transition behavior is not changing too much as shown in Figure 4b. Our current results demonstrate the similar phenomena as the ion-liquid gated VO_2-based FET devices by the way of p−n junction under the inverse bias voltage.

1. CONCLUSION

High-quality VO_2 epitaxial crystal films have been prepared by oxide-MBE method on p-type GaN/sapphire substrate to form an idea p−n junction. This junction displayed clear rectifying characteristics at room temperature and shown Schottkey contact above the phase transition temperature of VO_2 layer. By applying a bias voltage to the p−n junction, we achieved a phase transition modulation of the VO_2 film through a carrier/electron density control. Calculations of the barrier width/depletion layer at the interface as the function of the bias voltage, point out that for the thinner VO_2 epitaxial film, the phase transition modulation is effective and a metallic phase can be achieved at room temperature with a small inverse bias voltage. Furthermore, this bias voltage-assisted phase transition control exhibits a clear resistance switching behavior for the VO_2 layer, with potential applications in a logical memory or in sensor devices.

This work shows the possibility of achieving a phase transition control of VO_2 thin films through a p−n junction. The mechanism may allow the investigation of novel phase transitions mechanisms tuned with an external voltage. It offers also novel opportunities to implement Mott transistors, narrow gap semiconductor infrared detectors, or investigation of the low-dimensional correlated electron behavior.

ASSOCIATED CONTENT

Supporting Information

Synchrotron-based X-ray reflectometry (XRR) for the VO_2 layer on GaN/sapphire substrate and the carrier distribution schemes for the p−n junction under the conditions of the balance state, adding forward bias and reverse bias states, respectively. This material is available free of charge via the Internet at http://pubs.acs.org/.

AUTHOR INFORMATION

Corresponding Authors

*E-mail: czou@ustc.edu.cn.
*E-mail: wuzy@ustc.edu.cn.

Present Address

[§] Key Laboratory of Materials Modification by Laser, Ion, and Electron Beams (Ministry of Education), Dalian University of Technology, Dalian 116024, China.

Notes

The authors declare no competing financial interest.

ACKNOWLEDGMENTS

This work was partially supported by the National Basic Research Program of China (2012CB825800 and 2014CB848900), the Science Fund for Creative Research Groups of NSFC (11321503), the National Natural Science Foundation of China (11175183, U1432249), the Fundamental Research Funds for the Central Universities (WK2310000035), and the Opening Project of Key Laboratory of Materials Modification by Laser, Ion and Electron Beams, Ministry of Education (Project No.LABKF1401). The authors acknowledge the supporting from Shanghai Synchrotron Radiation Facility.

REFERENCES

(1) Morin, F. J. Oxides which Show a Metal-to-Insulator Transition at the Néel Temperature. *Phys. Rev. Lett.* **1959**, *3*, 34−36.

(2) Zhou, J. D.; Gao, Y.; Zhang, Z.; Luo, H.; Cao, C.; Chen, Z.; Dai, L.; Liu, X. VO_2 Thermochromic Smart Window for Energy Savings and Generation. *Sci. Rep.* **2013**, *3*, 3029.

(3) Huang, W. X.; Yin, X. G.; Huang, C. P.; Wang, Q. J.; Miao, T. F.; Zhu, Y. Y. Optical Switching of a Metamaterial by Temperature Controlling. *Appl. Phys. Lett.* **2010**, *96*, 261908.

(4) Driscoll, T.; Kim, H. T.; Chae, B. G.; Kim, B. J.; Lee, Y. W.; Jokerst, N. M.; Palit, S.; Smith, D. R.; Ventra, M. D.; Basov, D. N. Memory Metamaterisls. *Science* **2009**, *325*, 1518−1521.

(5) Li, Z.; Hu, Z.; Peng, J.; Wu, C.; Yang, Y.; Feng, F.; Gao, P.; Yang, J.; Xie, Y. Ultrahigh Infrared Photoresponse from Core-Shell Single-Domain VO_2/V_2O_5 Heterostructure in Nanobeam. *Adv. Funct. Mater.* **2014**, *24*, 1821−1830.

(6) Yang, Z.; Ko, C.; Ramanathan, S. Oxide Electronics Utilizing Ultrafast Metal-Insulator Transitions. *Annu. Rev. Mater. Res.* **2011**, *41*, 337−367.

(7) Han, Y. H.; Kim, K. T.; Shin, H. J.; Moon, S.; Choi, I. H. Enhanced Characteristics of an Uncooled Microbolometer Using Vanadium-Tungsten Oxide as a Thermometric Material. *Appl. Phys. Lett.* **2005**, *86*, 254101.

(8) Gu, Q.; Falk, A.; Wu, J.; Ouyang, L.; Park, H. Current-Driven Phase Oscillation and Domain-Wall Propagation in $W_xV_{1-x}O_2$ Nanobeams. *Nano Lett.* **2007**, *7*, 363−366.

(9) Batista, C.; Ribeiro, R. M.; Teixeira, V. Synthesis and Characterization of VO_2-Based Thermochromic Thin Tilms for Energy-Efficient Windows. *Nanoscale Res. Lett.* **2011**, *6*, 301.

(10) Takami, H.; Kanki, T.; Ueda, S.; Kobayashi, K.; Tanaka, H. Filling-Controlled Mott Transition in W-Doped VO_2. *Phys. Rev. B* **2012**, *85*, 205111.

(11) Wu, Y.; Fan, L.; Huang, W.; Chen, S.; Chen, C.; Chen, F.; Zou, C.; Wu, Z. Depressed Transition Temperature of $W_xV_{1-x}O_2$: Mechanistic Insights from the X-Ray Absorption Fine Structure (XAFS) Spectroscopy. *Phys. Chem. Chem. Phys.* **2014**, *16*, 17705−17714.

(12) Muraoka, Y.; Hroi, Z. Metal-Insulator Transition of VO_2 Thin Films Grown on TiO_2 (001) and (110) substrates. *Appl. Phys. Lett.* **2002**, *80*, 583−585.

(13) Quackenbush, N. F.; Tashman, J. W.; Mundy, J. A.; Sallis, S.; Paik, H.; Misra, R.; Moyer, J. A.; Guo, J. H.; Fischer, D. A.; Woicik, J. C.; Muller, D. A.; Schlom, D. G.; Piper, L. F. Nature of the Metal Insulator Transition in Ultrathin Epitaxial Vanadium Dioxide. *Nano Lett.* **2013**, *13*, 4857−4861.

(14) Aetukuri, N. B.; Gray, A. X.; Drouard, M.; Cossale, M.; Gao, L.; Reid, A. H.; Kukreja, R.; Ohldag, H.; Jenkins, C. A.; Arenholz, E.; Roche, K. P.; Dürr, H. A.; Samant, M. G.; Parkin, S. S. P. Control of the Metal-Insulator Transition in Vanadium Dioxide by Modifying Orbital Occupancy. *Nat. Phys.* **2013**, *9*, 661−666.

(15) Shibuya, K.; Tsutsumi, J.; Hasegawa, T.; Sawa, A. Fabrication and Raman Scattering Study of Epitaxial VO_2 Thin Films on MgF_2 (001) Substrates. *Appl. Phys. Lett.* **2013**, *103*, 021604.

(16) Fan, L. L.; Chen, S.; Luo, Z. L.; Liu, Q. H. L.; Wu, Y. F.; Song, L.; Ji, D. X.; Wang, P.; Chu, W. S.; Gao, C.; Zou, C. W.; Wu, Z. Y. Strain Dynamics of Ultrathin VO_2 Fil Grown on TiO_2 (001) and the Associated Phase Transition Modulation. *Nano Lett.* **2014**, *14*, 4036−4043.

(17) Ji, H.; Wei, J.; Natelson, D. Modulation of the Electrical Properties of VO_2 Nanobeams Using an Ionic Liquid as a Gating Medium. *Nano Lett.* **2012**, *12*, 2988−2992.

(18) Nakano, M.; Shibuya, K.; Okuyama, D.; Hatano, T.; Ono, S.; Kawasaki, M.; Iwasa, Y.; Tokura, Y. Collective Bulk Carrier Delocalization Driven by Electrostatic Surface Charge Accumulation. *Nature* **2012**, *487*, 459−462.

(19) Jeong, J.; Aetukuri, N.; Graf, T.; Schladt, T. D.; Samant, M. G.; Parkin, S. S. P. Suppression of Metal-Insulator Transition in VO_2 by Eletric Field-Induced Oxygen Vacancy Formation. *Science* **2013**, *339*, 1402−1405.

(20) Tan, X. G.; Yao, T.; Long, R.; Sun, Z. H.; Feng, Y. J.; Cheng, H.; Yuan, X.; Zhang, W. Q.; Liu, Q. H.; Wu, C. Z.; Xie, Y.; Wei, S. Q. Unraveling Metal-Insulator Transition Mechanism of VO_2 Triggered by Tungsten Doping. *Sci. Rep.* **2012**, *2*, 466.

(21) Yin, H.; Luo, M.; Yu, K.; Gao, Y.; Huang, R.; Zhang, Z.; Zeng, M.; Cao, C.; Zhu, Z. Fabrication and Temperature-Dependent Field-Emission Properties of Bundlelike VO_2 Nanostructure. *ACS Appl. Mater. Interfaces* **2011**, *3*, 2057−2062.

(22) Ko, C.; Yang, Z.; Ramanathan, S. Work Function of Vanadium Dioxide Thin Films Across the Metal-Insulator Transition and the Role of Surface Nonstoichiometry. *ACS Appl. Mater. Interfaces* **2011**, *3*, 3396−3401.

(23) Sohn, A.; Kim, H.; Kim, D. W.; Ko, C.; Ramanathan, S.; Park, J.; Seo, G.; Kim, B. J.; Shin, J. H.; Kim, H. T. Evolution of Local Work Function in Epitaxial VO_2 Thin Films Spanning the Metal-Insulator Transition. *Appl. Phys. Lett.* **2012**, *101*, 191605.

(24) Martens, K.; Radu, I. P.; Mertens, R. S.; Shi, X.; Nyns, L.; Cosemans, S.; Favia, P.; Bender, H.; Conard, T.; Schaekers, M.; Gendt, S. D.; Afanas'ev, V.; Kittl, J. A.; Heyns, M.; Jurczak, M. The VO_2 Interface, the Metal-Insulator Transition Tunnel Junction, and the Metal-Insulator Transition Swithch On-Off Resistance. *J. Appl. Phys.* **2012**, *112*, 124501.

(25) Rosevear, W. H.; Paul, W. Hall-Effect in VO_2 Near the Semiconductor-to-Metal Transition. *Phys. Rev. B* **1973**, *7*, 2109−2111.

(26) Ruzmetov, D.; Heiman, D.; Claflin, B. B.; Narayanamurti, V.; Ramanathan, S. Hall Carrier Density and Magneto Resistance Measurements in Thin-Film Vanadium Dioxide across the Metal-Insulator Transition. *Phys. Rev. B* **2009**, *79*, 153107.

(27) Zhou, Y.; Ramanathan, S. GaN/VO_2 Heteroepitaxial p-n Junctions: Band Offset and Minority Carrier Dynamics. *J. Appl. Phys.* **2013**, *113*, 213703.

(28) Zhou, Y.; Ramanathan, S. Heteroepitaxial VO_2 Thin Films on Gan: Structure and Metal-Insulator Transition Characteristics. *J. Appl. Phys.* **2012**, *112*, 074114.

(29) Fan, L. L.; Chen, S.; Wu, Y. F.; Chen, F. H.; Chu, W. S.; Chen, X.; Zou, C. W.; Wu, Z. Y. Growth and Phase Transition Characteristics of Pure M-phase VO_2 epitaxial Film Prepared by Oxide Molecular Beam Epitaxy. *Appl. Phys. Lett.* **2013**, *103*, 131914.

(30) Lei, T.; Ludwig, K. F.; Moustakas, T. D. Heteroepitaxy, Polymorphism, and Faulting in Gan Thin Films on Silicon and Sapphire Substrates. *J. Appl. Phys.* **1993**, *74*, 4430−4437.

(31) Gupta, A.; Narayan, J.; Dutta, T. Near Bulk Semiconductor to Metal Transition in Epitaxial VO_2 Thin Films. *Appl. Phys. Lett.* **2010**, *97*, 151912.

(32) Fan, L. L.; Wu, Y. F.; Si, C.; Zou, C. W.; Qi, Z. Q.; Li, L. B.; Pan, G. Q.; Wu, Z. Y. Oxygen Pressure Dependent VO_2 Crystal Film Preparation and the Interfacial Epitaxial Growth Study. *Thin Solid Films* **2012**, *520*, 6124−6129.

(33) Zhang, S.; Kim, I. K.; Lauhon, L. J. Stoichiometry Engineering of Monoclinic to Rutile Phase Transition in Suspenden Single Crystalline Vanadium Dioxide Nanobeams. *Nano Lett.* **2011**, *11*, 1443−1447.